Intra-Frame Bidirectional Transmission in Networks of Visible LEDs

Qing Wang, *Student Member, IEEE*, and Domenico Giustiniano, *Member, IEEE*

***Abstract*— The optical antenna's directionality of nodes forming a visible light communication (VLC) network, i.e., their field-of-view (FOV), varies greatly from device to device. This encompasses wide FOVs of ambient light infrastructure and directional FOVs of light from low-end embedded devices. This variety of light propagation can severely affect the transmission reliability, despite pointing the devices to each other may seem enough for a reliable communication. The presence of interference among nodes with different FOVs makes traditional access protocols in VLC unreliable, and it also exacerbates the hidden-node problem. In this paper, we propose a carrier sensing multiple access/collision detection and hidden avoidance (CSMA/CD-HA) medium access control protocol for a network, where each node solely uses one light-emitting diode to transmit and receive data. The CSMA/CD-HA can enable in-band intra-frame bidirectional transmission with just one optical antenna. The key idea is to exploit the intra-frame data symbols without the emission of light to introduce an embedded communication channel. This approach enables the transmission of additional data while receiving in the same optical frequency band, and it makes the communication robust to different types of FOVs. We implement the CSMA/CD-HA protocol in a software-defined embedded platform running Linux, and evaluate its performance through analysis and experiments. Results show that collisions caused by hidden nodes can largely be reduced, and our protocol can increase the saturation throughput by nearly up to 50% and 100% under the two- and four-node scenarios, respectively.**

***Index Terms*— Visible light communication, bidirectional transmission, MAC protocol, analysis, design, implementation.**

I. Introduction

VISIBLE Light Communication (VLC) is emerging as a complementary technology to mainstream research on Radio Frequency (RF) communication. VLC utilizes visible light from Light Emitting Diodes (LEDs) to convey digital information between devices. A network of visible LEDs could be enabled by connecting various devices such as ceiling bulbs, lamps, light emitters embedded into cars and mobile devices and perhaps, in the future, LED TVs. However, the directionality of the optical antenna of VLC, i.e., the Field Of View (FOV) of LEDs, varies greatly from device to device. An infrastructure, e.g., a light bulb on the ceiling, normally emits light with a wide-FOV. In contrast, mobile devices may have various FOVs, according to the space and power constraints.

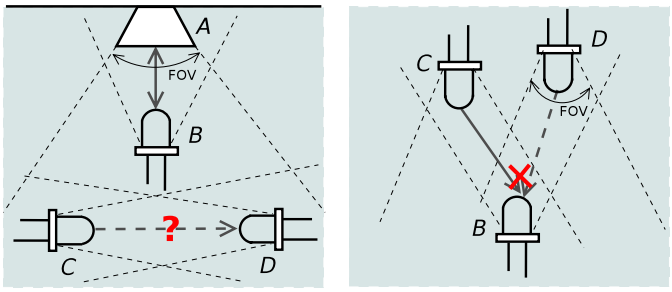

Fig. 1. Motivation – various directionality of the optical antenna of VLC nodes and OOK modulation: *left)* is in-band interference-free concurrent transmissions of $A \leftrightarrow B$ and $C \rightarrow D$ possible? *right)* exacerbate the hidden-node problem.

This variety of light wave propagation calls for networking approaches that are robust to the specific optical antenna. The design opportunities can take advantage of two fundamental differences with respect to RF communication.

- First, VLC often adopts the On-Off Keying (OOK) modulation or the Variable Pulse Position Modulation (VPPM), thus a transmitter can be "idle" (doest not need to emit light) when transmitting an "OFF" signal. This implies that *other communications could be established during these short times without light emission*. These concurrent communications may improve the system performance, such as increasing the throughput and so on.
- Second, while photodiodes are normally used as receivers, a LED has been proved to work as a receiver in LED-to-LED communications [2], [3]. Thus, a network of LEDs would only require one LED as optical antenna at each transceiver. The challenge is then how to create a network of LEDs *with* different FOVs and *without* additional optical components.

As illustrated in Fig. 1, these differences i) bring opportunities to design new Medium Access Control (MAC) protocols to improve the network performance; ii) increase the hidden-node problem in some scenarios. In this paper, we propose a Carrier Sensing Multiple Access/Collision Detection&Hidden

Manuscript received April 29, 2015; revised January 3, 2016; accepted February 12, 2016; approved by IEEE/ACM TRANSACTIONS ON NETWORKING Editor T. Hou. This work was supported in part by the Ministerio de Economía y Competitividad under Grant TEC2014-55713-R and in part by the Madrid Regional Government through the TIGRE5-CM Program under Grant S2013/ICE-2919. Preliminary results were presented at the 2014 ACM Conference on Emerging Networking Experiments and Technologies [1]. *(Corresponding author: Qing Wang.)*

Q. Wang is with the IMDEA Networks Institute, 28918 Leganes (Madrid), Spain, and also with the University Carlos III of Madrid, 28918 Leganes (Madrid), Spain (e-mail: qing.wang@imdea.org).

D. Giustiniano is with the IMDEA Networks Institute, 28918 Leganes (Madrid), Spain (e-mail: domenico.giustiniano@imdea.org).

Color versions of one or more of the figures in this paper are available online at http://ieeexplore.ieee.org.

Digital Object Identifier 10.1109/TNET.2016.2530874

Avoidance (CSMA/CD-HA) MAC protocol to enable intra-frame bidirectional VLC in a network of LEDs. Similarly to the emerging full-duplex of RF communications with a single antenna proposed by [4], CSMA/CD-HA only uses one antenna – a single LED to enable in-band bidirectional communication. In contrast to full-duplex research in RF domain, we target visible light spectrum and implement very simple techniques to enable intra-frame bidirectional communication with off-the-shelf credit-card-sized embedded board with a total unit cost (including the VLC transceiver) of approximately 50 dollars.

By enabling in-band bidirectional transmissions, the proposed mechanism can improve the system saturation throughput. In ad-hoc networks, the proposed CSMA/CD-HA protocol can shorten the average frame collision time as well as alleviate the hidden-node problem without using the Request-To-Send/Clear-To-Send (RTS/CTS) method, thus improving the system performance in terms of frame collision probability and throughput. We evaluate the performance of our protocol from analysis and experiments. For the experimental evaluation, we implement the CSMA/CD-HA protocols and underlying techniques in a software-defined embedded platform running Linux. Experimental results show that the proposed protocol can increase the saturation throughput by nearly up to 50% and 100% in a two- and four-node networks, respectively. In ad-hoc networks, shortened frame collision time is demonstrated by the experimental evaluation. The hidden-node problem is also alleviated greatly, and the system throughput is improved significantly. Practical issues for the implementation, such as the robustness to the data pattern of the payload, are also addressed and solved.

The rest of this paper is organized as follows. Related work is summarized in Sec. II. Fundamental designs of the intra-frame bidirectional transmission and the proposed CSMA/CD-HA protocol are presented in Sec. III, followed by the analysis and numerical results in Sec. IV. Details of the implementation in an embedded platform and the performance evaluations are given in Sec. V and Sec. VI, respectively. Conclusions are drawn in Sec. VII.

II. Related Work

VLC has received strong attention from designers of next generation cellular networks [5], [6], the point-to-point communication using smartphone [7], [8] and cars [9], [10]. Using visible light to enable indoor localization [11]–[13], light-to-camera [7], [8], [11], [12], [14] and screen-to-camera [8], [15], [16] communications are also well investigated. Besides, the IEEE has developed the 802.15.7 standard [17] for short-range communication with visible light.

Single Antenna VLC: While photodiodes are normally used as receivers, a reverse-biased LED instead of a photodiode was used in [2] as a receiver to implement a bidirectional communication network. This principle had been exploited by [3] to introduce a low-power LED-to-LED communication network. This work operated on microcontrollers and was implemented as embedded software in the environment of non-operating system. Connecting it with various networking protocols is not straightforward. In contrast, we have designed and implemented OpenVLC [18]–[20] (`www.openvlc.org`), an open-source software-defined platform for VLC networks. OpenVLC is built around a low-cost embedded Linux platform. Its software-defined solution is implemented as a Linux driver and thus it appears as a normal network interface that can easily interoperate with Internet protocols. Recently, authors in [21] investigated the feasibility of adopting a commercial high-power LED as a transceiver. They demonstrated a system that achieves a PHY layer rate of 15 Mb/s with the OOK modulation.

Full-Duplex RF/VLC Communication: In-band full-duplex RF communication was proposed in [22] and further implemented as a prototype in [23]. The key technique is a device that uses the inverse of its transmitted signals to cancel the self-interference to its received signal. Compared to our proposed technique, both of them can achieve in-band bidirectional transmission. A different is that [22] and [23] used two antennas for both transmitting and receiving, while in our technique, a single LED is used for that purpose. Recently, a method combining analog and digital cancellation is proposed in [4]. This method enables the full duplex communication with a single antenna. For full-duplex VLC, some authors propose to use visible and infrared lights or LEDs operating on different wavelengths for full-duplex transmission, as in [24]. Furthermore, the authors in [25] propose to use an isolator between the LED and photodiode at each node for full-duplex VLC, and claim the mutual interference between the bidirectional LED-to-photodiode links is negligible. Compared to these work, we only need a single LED at each node to implement an in-band interference-free full-duplex VLC system.

A preliminary version of this paper was presented in [1]. Compared to our previous work, in this paper we further model and analyze the proposed protocol. Besides, we improve the protocol design and system implementation, evaluate the system in new experimental tests, and the performance has been improved by nearly a factor of ten. We also introduce Reed-Solomon error correction and bit scrambling to achieve more robust performance of the system under different scenarios.

III. System Design

We first briefly introduce background information on coding and decoding schemes adopted in this work. Then we present the key technique at symbol level to enable intra-frame bidirectional transmission in a network of visible LEDs, where a single LED is used as optical antenna at each transceiver (without additional optical components). Finally we propose a MAC protocol to exploit this technique at system level.

A. Coding/Decoding Schemes

We use intensity modulation for data transmission, which is also adopted by the IEEE 802.15.7 standard developed for short-range communication using visible light of wideband light bulbs [17]. Binary information is mapped to the presence

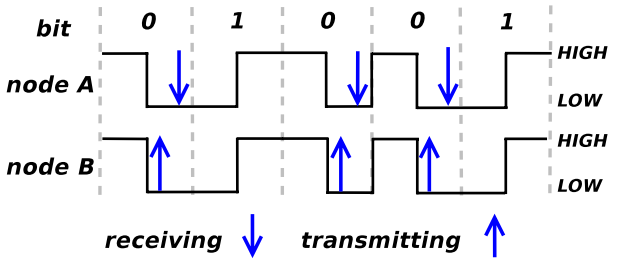

Fig. 2. The key technique at symbol level that enables intra-frame bidirectional transmission. Nodes can switch with symbol-level granularity between transmitting and receiving. In the example with Manchester code, node A can receive one symbol when it transmits the symbol LOW of bit "0" of the line code. In more general terms, the intra-frame bidirectional transmission can be enabled for those symbols where there is a probability of one to jump to a state where node A transmits the symbol LOW.

(symbol HIGH) or absence (symbol LOW) of the visible light carrier. The main physical layer of the IEEE 802.15.7 standard uses the OOK modulation with the Manchester Run-Length Limited (RLL) line code. RLL line codes are used to avoid long runs of light on and light off that could end up in flicker effects, as well as clock and data recovery detection problems. Therefore, in our system bit 1 is mapped to symbol sequence LOW-HIGH, and bit 0 is mapped to HIGH-LOW. Demodulation is performed with direct detection. Based on the received signal's voltage, the receiving node detects the received signal as the sequence of symbols HIGH and LOW that are then converted to binary data.

B. Key Technique at Symbol Level

The key enabler of the intra-frame bidirectional transmission technique is that a node normally does not need to emit light when transmitting a symbol LOW. Thanks to this, nodes could switch between being a transmitter and a receiver with symbol-level granularity during a frame transmission.

Let us consider an example of the communication between two nodes, A and B. We assume that node A transmits data to node B. *Node A is "idle" when it transmits a symbol LOW, and it can make use of this time to receive a data symbol.* To cooperate with this, node B can start itself to transmit a symbol if it can *predict* that it will receive a symbol LOW in the next symbol slot. We illustrate an example in Fig. 2. For the Manchester RLL code used in this paper, the prediction is based on:

- node B receives a symbol HIGH in current symbol slot;
- the symbol HIGH is the first part of a modulated bit (i.e., bit "0").

Just equipped with one LED, node B can switch to send data during the reception of a frame, while node A can switch to receive data when it transmits a frame. This switching between a transmitter and a receiver at symbol level allows for in-band bidirectional symbol transmission.

As shown in Fig. 2, node A may expect to receive a symbol only when it transmits the symbol LOW of bit "0". The reason is that node B can only predict the symbol LOW of bit "0", but it can not predict the symbol LOW of bit "1". In expectation, half of data from node A are with bit "1" and the other half with bit "0". Therefore, node B will transmit data for half of the payload of node A.

This approach can be extended to other RLL line codes. In more general terms: the intra-frame bidirectional transmission can be enabled for those symbols that there is a probability of one to jump to a state where node A transmits a symbol LOW.

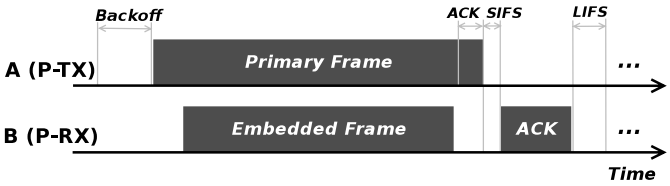

Fig. 3. CSMA/CD-HA MAC protocol with a primary transmitter and a primary receiver. *(Note: the DATA/ACK frames shown here are transmitted by their corresponding nodes, not received.)*

TABLE I
NOTATIONS USED IN THE PROPOSED MAC PROTOCOL

Notation	Explanation
Primary TX (P-TX)	Node that has gained access to the medium by backoff protocol
Primary RX (P-RX)	Peer RX of a P-TX
Secondary TX (S-TX)	Node (not P-RX) sending an in-band frame with the P-TX's transmission
Secondary RX (S-RX)	Peer RX of a S-TX
Primary frames	Frames sent by a P-TX to a P-RX
Embedded frames	Frames sent opportunistically by either a P-RX or a S-TX
Embedded channels	The in-band communication channels where embedded frames are transmitted

C. The CSMA/CD-HA MAC Protocol

The Carrier Sensing Multiple Access/Collision Detection& Hidden Avoidance (CSMA/CD-HA) protocol is proposed to ensure fair channel access among all VLC nodes and reduce the impact of collisions and hidden nodes. When introducing our protocol, we refer to Fig. 3 for the illustration of the protocol and to Table I for the short notations.

When a frame is available for transmission, the MAC first senses the channel. The frame is transmitted immediately if the channel is sensed clear. If the channel is assessed busy, the MAC starts a backoff counter. The frame is transmitted when the counter reaches zero. The transmitting node and its corresponding receiver become a primary transmitter (P-TX) and a primary receiver (P-RX), respectively. Based on the symbol-level technique introduced in Sec. III-B:

- The P-TX switches to receiving mode during the transmission of the primary frame when it transmits the symbols LOW of bit "0", waiting to receive the symbols of an embedded frame.
- The P-RX prepares an embedded frame if it decodes that it is the intended receiver of the primary frame. Every time the P-RX receives a symbol HIGH of bit "0" (thus predicting that the next incoming symbol is LOW), it switches to transmission mode and it sends a symbol of the embedded frame through the embedded channel.

In this way, the intra-frame bidirectional transmission is enabled. Note that the P-RX should transmit the whole embedded frame before the P-TX finishes to transmit the primary frame.

After the P-TX successfully receives the embedded frame, it appends an-octet ACK to the primary frame it is transmitting to acknowledge the reception of embedded data. If the P-RX decodes the frame successfully, it sends an ACK to the P-TX after a duration of Short Inter-Frame Space (SIFS) since it receives the primary frame. After the transmission of the ACK finishes, nodes restart to compete the channel access after a Long Inter-Frame Space (LIFS) period. If the P-TX has not received an ACK within the timeout, a retransmission occurs and the contention window is doubled unless it reaches the maximal contention window. A frame is dropped when a pre-defined number of retransmissions fail.

D. Main Features of the CSMA/CD-HA Protocol

In this part, we present the main features of the CSMA/CD-HA protocol. First, *the CSMA/CD-HA protocol has the ability to alleviate hidden nodes.* As a result of intra-frame bidirectional transmission, the P-RX will transmit embedded symbols when it is the intended receiver of a communication initiated by the P-TX. Part of these symbols are HIGH. These symbols HIGH (corresponding to transmission of light) can be sensed by the nodes under its coverage, thus they will not send frames to the receiver during this period and the potential hidden-node problem is alleviated. The only part of the frame which is not protected to hidden nodes is before the embedded frames start to be transmitted, when a hidden node to the TX may judge the channel as clear. However, this duration is usually short compared to the whole frame transmission period and the influence tends to be very low. Sometimes the P-RX may have no data to transmit. Under this case, it can send dummy symbols to announce that the channel is busy while it is receiving a frame. To summarize, the embedded frames of the primary communication in the CSMA/CD-HA protocol have twofold use: send additional in-band data and act as active acknowledgement of ongoing primary data reception to protect the primary transmitter from hidden nodes.

CSMA/CD-HA Is Also Useful for Collision Detection: Traditional collisions caused by nodes reaching the back-off counter equal to zero are still possible. Collisions may also occur when hidden nodes start transmitting before the P-RX's transmission of an embedded frame, as described in the previous paragraph. *These collisions are detectable if the P-RX receives the HIGH-HIGH sequence (which is invalid) for a pre-defined certain times.* Details of the collision detection at P-RX is presented in Algorithm 1.[1] Upon a collision detected by P-RX (lines 7-9 of Algorithm 1), P-RX stops transmitting embedded data if the transmission of the embedded frame was ongoing, or otherwise it does not start the transmission of an

Algorithm 1 Collision Detection at the P-RX

Input: `txSymb`: to-be-transmitted symbol; `numErr`: the current amount of received invalid sequences; `maxNumErr`: the threshold of `numError`.
Output: collision detected: **true / false**; `rxSymb`: the received symbol; `numError`: updated.

```
1: if txSymb is HIGH then
2:   transmit symbol txSymb to the P-TX
3:   rxSymb ← LOW
4: else
5:   rxSymb ← receive a symbol from the P-TX
6:   # If P-RX receives an invalid HIGH-HIGH sequence
7:   if rxSymb is HIGH && (++numErr) > maxNumErr
     then
8:     return true   # collision detected
9:   end if
10: end if
11: return false   # no collision
```

Algorithm 2 Collision Detection at the P-TX

Input: `numLOW`: the current amount of continuously received symbols LOW; `maxNumLOW`[2]: the threshold of `numLOW`.
Output: collision detected: **true / false**; `rxSymb`: the received symbol; `numLOW`: updated.

```
1: rxSymb ← receive a symbol from the P-RX
2: if rxSymb is LOW then
3:   if (++numLOW) > maxNumLOW then
4:     return true   # collision detected
5:   end if
6: else
7:   numLOW ← 0
8: end if
9: return false   # no collision
```

embedded frame. Consequently, *this collision can be detected by P-TX due to the absence of embedded transmission from P-RX*. The detection details are shown in Algorithm 2, which is executed by P-TX after it transmits the symbol HIGH of a modulated bit "0" (no need to emit light to transmit the following symbol LOW). If a collision is detected (lines 3-5 of Algorithm 2), the ongoing primary frame transmission will be terminated by the P-TX immediately without waiting for the end of the payload, which increases the channel utilization.

Finally, *secondary intra-frame concurrent transmission can also be enabled,* depending on the number of existing nodes, the FOVs of their LEDs and their positions. Take the left scenario in Fig. 1 as an example. The wide-FOV LEDs of node A make it possible to communicate with nodes B, C, and D, while the latter three have limited connectivity due to their narrow-FOV LEDs. We illustrate an example of the protocol in Fig. 4. Nodes C and D can receive A's signals, and C can detect that it is not (as well as D) the intended receiver

[1]Note that the algorithm is only called by the P-RX when i) it receives a symbol HIGH in the previous symbol slot and ii) it infers that the symbol HIGH is the first part of a modulated bit.

[2]The `maxNumLOW` is initiated based on experience, and then is updated on per-frame basis to be twice of the maximal continuous "0" in the latest received frame.

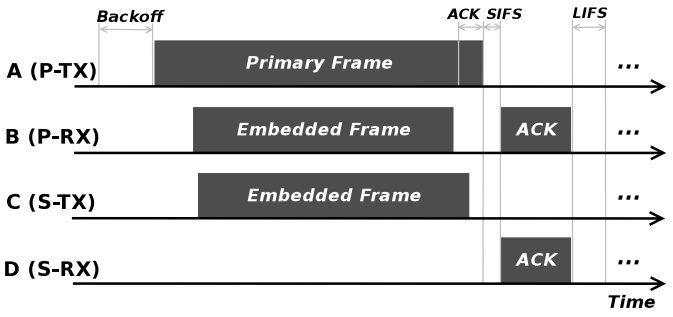

Fig. 4. CSMA/CD-HA MAC protocol that supports intra-frame bidirectional transmission: an illustration of concurrent transmissions for the left scenario of Fig. 1. *(Note: the DATA/ACK frames shown here are transmitted by their corresponding nodes, not received.)*

of data from A. Node C then transmits embedded frames to D as node B transmits to A (C thus becomes a S-TX), while D can receive these frames following exactly A's receiving steps (D thus becomes a S-RX). After successfully decoding a frame from node C, D sends back an ACK when the transmission of the primary frame is finished. The transmission of ACK from node D to C will not cause any interference to the communication between nodes A (the P-TX) and B (the P-RX).

E. Discussion

We continue to discuss some other important aspects of the proposed protocol.

Length of an Embedded Frame: The length of an embedded frame heavily depends on the number of bit "0"s in the primary frame body. This number can be calculated by the transmitter P-TX based on its payload and appended to the MAC frame header. Note that this appended number only serves as a reference. The actual length of an embedded frame also depends on when the P-RX/S-TX starts transmitting an embedded frame. The P-RX/S-TX calculates the length of embedded frame by subtracting L from the reference number suggested by P-TX, where L is the amount of information P-RX/S-TX can transmit during the time interval between the transmissions of primary and embedded frames by the P-TX and P-RX/S-TX, respectively. The L increases if P-RX/S-TX spends longer time for the backoff process on competing the secondary channel.

When to Send an Embedded Frame: An embedded frame should be transmitted after a node receives the source address of the current primary frame. Only the intended receiver of the transmission can be declared as P-RX. Other nodes may act as S-TX, as long as they are not the intended receivers of P-RX. They start a secondary backoff process that follows the same rules as the primary one to decide the access to the medium.

Robustness of Intra-Frame Concurrent Transmissions: The intra-frame current transmissions should be robust to expected or unexpected events, i.e., the secondary transmission should be disabled immediately if the primary transmission stops due to detections of collisions or hidden nodes or other unexpected errors. The CSMA/CD-HA protocol has this ability. For example, an underlying assumption of secondary transmissions is that the FOVs of nodes is such that the transmission of S-TX and S-RX does not interfere with the transmission of P-TX and P-RX. If this is not the case, the primary transmission is stopped due to detected collisions. As soon as P-TX stops its transmission because of a detected collision, the secondary transmission of S-TX and S-RX will be disabled for a while.

Intra-Frame Bidirectional Transmission Between S-TX and S-RX: In our current protocol design, S-RX does not predict "LOW" symbols transmitted by S-TX, to reduce complexity. Therefore, the transmission between S-TX and S-RX is not intra-frame bidirectional, and S-TX could not detect collisions during its transmission of an embedded frame. In principle, however, collision detection by S-TX and the intra-frame bidirectional transmission between S-TX and S-RX are feasible assuming that S-TX adopts a similar modulation scheme (e.g., OOK + Manchester RLL code) as P-TX does.

IV. Throughput Analysis

In this section, we analyze the system performance of the CSMA/CD-HA protocol in terms of saturation throughput. We first consider a simplified CSMA/CD-HA protocol to analyze the performance improvement from embedded channels by enabling the intra-frame bidirectional transmission. After that, we analyze the performance of the CSMA/CD-HA protocol in common ad-hoc scenarios.

A. Performance With Embedded Channels

To analyze the performance improvement from embedded channels, we first adopt *a simplified CSMA/CD-HA protocol where the backoff mechanism is disabled*. We consider a network consisting of an access point (AP) equipped with wide FOV LEDs and N users with narrow FOV LED, similar to the scenario presented in Fig. 1(left). All the users are under the AP's coverage and therefore can detect the data it transmits in the same frequency band of the visible light spectrum. During the AP's transmission, the users can opportunistically send data to the AP or to other users through the embedded channels as presented in Sec. III. To simplify the derivation, *we assume that the AP always has access to the channel and it keeps sending data to users, and other users can only transmit data through embedded channels.*

To derive the saturation throughput of this system, we first make some notations. Let T_h denote the time to transmit the frame header, and $E[T_p]$ be the average time for the transmission of frame payload. The intervals of SIFS and LIFS are denoted as T_s and T_l, respectively. Moreover, let T_a be the time to transmit an ACK and δ be the propagation delay. We assume there is no error in the PHY layer transmission. Then the total time T_f to transmit a frame can be written as

$$T_f = T_h + E[T_p] + \delta + T_s + T_a + \delta + T_l \tag{1}$$

Let us assume the AP serves the users alternately. Let $E[L_p]$ denote the average effective payload of a primary frame,

and S_{wo} be the system saturation throughput without embedded channels. Then S_{wo} can be written as

$$S_{wo} = N \cdot \frac{E[L_p]}{N \cdot T_f} = \frac{E[L_p]}{T_f} \tag{2}$$

Similarly, let $E[L_{em}]$ be the average effective payload of embedded frames, and S_w denote the saturation throughput of a system with an average number of N_{em} embedded channels. We have

$$S_w = \frac{E[L_p] + N_{em} \cdot E[L_{em}]}{T_f}. \tag{3}$$

B. Ad-Hoc Scenario

We adopt the Markov chain model to analyze the performance of the CSMA/CD-HA protocol in ad-hoc networks. We consider a system consisting of N users and all the users can communicate with each other, *i.e.*, there are no *hidden nodes*. We assume all nodes always have data to transmit and we aim to derive the MAC layer saturation throughput of the system.

The classic Markov Chain model to analyze the performance of the Carrier Sense Multiple Access/Collision Avoidance (CSMA/CA) MAC protocol of IEEE 802.11 was introduced in [26], and then extended to many other different scenarios, *e.g.*, unsaturated traffic [27], hidden nodes scenario [28], and so on. The author in [26] adopted a two-dimension Markov chain to describe the 802.11 MAC operations. We also use this model for our system, but set a maximal retransmission times and assume that it is equal to the maximal backoff stage. A frame will be dropped if its retransmission times exceed the retransmission threshold. Following the derivation presented in the appendix, we can compute the saturation throughput of CSMA/CA, CSMA/CD (for one single optical antenna, and presented in [3]), and the CSMA/CD-HA (with embedded transmission) proposed in this work. Let S_{ca} denote the saturation throughput under CSMA/CA. Then S_{ca} can be written as

$$S_{ca} = \frac{P_f E[L_p]}{(1 - P_{tr})\sigma + P_f T_f + P_c T_c^{ca}} \tag{4}$$

where σ is the duration of an empty time slot. Similarly, let S_{cd} and S_{cd_ha} be the saturation throughputs under CSMA/CD and under CSMD/CD-HA (with embedded transmission), respectively. We have

$$S_{cd} = \frac{P_f E[L_p]}{(1 - P_{tr})\sigma + P_f T_f + P_c T_c^{cd}} \tag{5}$$

$$S_{cd\_ha} = \frac{P_f (E[L_p] + E[L_{em}])}{(1 - P_{tr})\sigma + P_f T_f + P_c T_c^{cd}}. \tag{6}$$

C. Numerical Results

In this part, we present some numerical results of our proposed protocols. The parameter settings used in the calculation are listed in Table II. The payloads of embedded frames L_{em} are set to the maximal lengths that can ensure the transmissions of embedded frames finish before those of primary frames. In addition, the Reed-Solomon (RS) error correcting code (232,200) is applied to all the primary and embedded frames.

TABLE II
PARAMETER SETTINGS IN THE ANALYSIS

Parameter	Value (unit)
N	2, 3, ..., 10
m	4
T_h	168 (optical clocks)
T_s, T_l, T_a	40, 120, 200 (optical clocks)
σ	0.001 (optical clocks)
L_p	50, 100, 200, 400, 600, 800, 1000 (bytes)
L_{em}	1, 20, 80, 180, 280, 380, 480 (bytes)

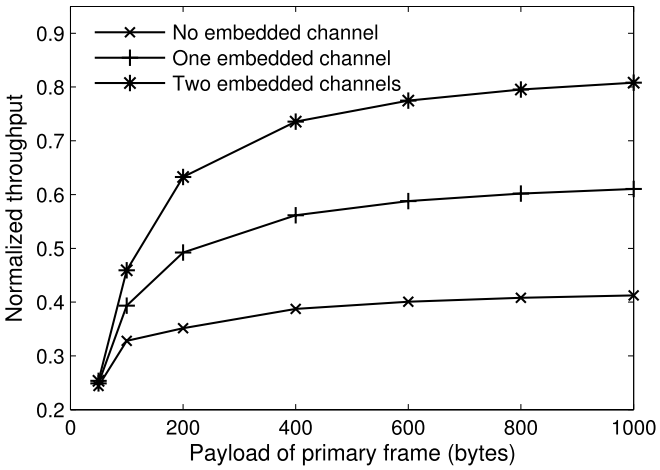

Fig. 5. Theoretical saturation throughput with embedded channels.

1) Performance With Embedded Channels: Without loss of generality, here we consider the scenario illustrated in Fig. 1(left). We compare the system saturation throughput under three different cases: i) without intra-frame bidirectional transmission (*i.e.*, no embedded channel); ii) with the intra-frame bidirectional transmission between nodes A and B (*i.e.*, one embedded channel, from node B to A); iii) with intra-frame bidirectional transmissions between nodes A and B, and the intra-frame unidirectional transmission from node C to D (i.e, two embedded channels, from node B to A, and from node C to D).

The normalized saturation throughputs versus the payload of primary frames are shown in Fig. 5. First we can observe that regardless of the number of embedded channels, the throughput increases consistently with the payload of primary frames, as expected. When the payload of primary frames is small (*e.g.*, 50 bytes), the embedded frames can hardly carry any payload. Thus the throughputs under all cases are similar to each other. We also observe that the throughput gains from embedded channels increase as the payload of primary frames increases. When the payload increases to 1000 bytes, the throughputs under one and two embedded channels can outperform that under no embedded channel by nearly 50% and 100%, respectively.

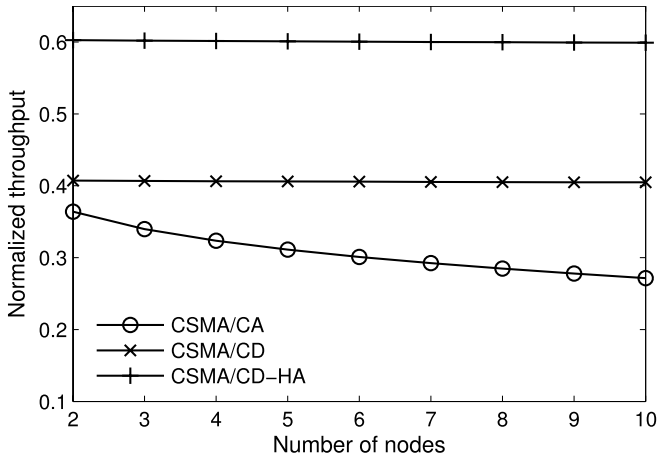

(a)

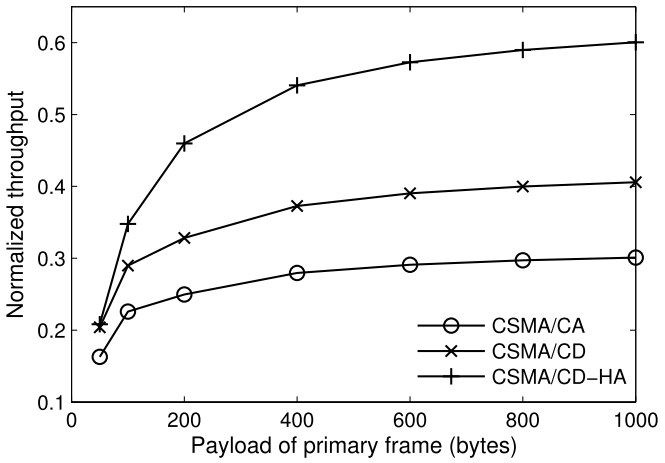

(b)

Fig. 6. Theoretical saturation throughput in ad-hoc networks. (a) Throughput vs. number of nodes. (b) Throughput vs. primary frame payload.

Besides, we can conclude from the figure that the throughput gain will increase greatly if there are more embedded channels enabled.

2) Ad-Hoc Scenario: We compare numerical results in ad-hoc networks under three different MAC protocols: i) the CSMA/CA protocol as described in [26]; ii) the CSMA/CD protocol [3]; iii) our proposed CSMA/CD-HA protocol with enabled intra-frame bidirectional transmission.

Fig. 6(a) shows the normalized saturation throughput versus the number of nodes. Those nodes compete with each other to access the shared channel. The payloads of each primary and embedded frames are fixed to 1000 and 480 bytes, respectively. We first observe that the throughput with CSMA/CA decreases gradually as the number of nodes increases, in accordance with the result shown in [26]. The reason behind those results is that the more nodes compete for the shared channel, the more time will be wasted on transmitting corrupted frames due to collisions. Instead, the throughputs with both CSMA/CD and CSMA/CD-HA are less sensitive to the number of competing nodes. This benefits from the fact that, with CSMA/CD and CSMA/CD-HA, the collisions can be timely detected and the transmissions of corrupted frames are stopped immediately, saving time from transmitting frames that would waste the shared resources. Thanks to the embedded channel, we can see from the figure that CSMA/CD-HA outperforms CSMA/CD by around $50\,\%$.

The normalized saturation throughput versus the payload of primary frames is shown in Fig. 6(b). The number of nodes is fixed to six. As expected, the throughputs with all protocols increase consistently with the payload. We can also observe that the throughputs of both CSMA/CD and CSMA/CD-HA are higher than that with CSMA/CA. Besides, the difference between CSMA/CD and CSMA/CD-HA increases as the payload increases, due to the longer payloads carried by embedded frames.

V. Implementation

We implement the proposed MAC protocol and the underlying symbol-level techniques in our general-purpose software-defined open source platform OpenVLC for visible light communication networks [19], [20]. The implementation is part of a new Linux driver that can communicate directly with the VLC hardware and the Linux networking stack.

A. Hardware

The OpenVLC platform consists of a BeagleBone Black (BBB) board[3] and a front-end transceiver. OpenVLC is based on three optical antennas: low-power LED, high-power LED and a photodiode. In this work, we consider one of the optical antennas of the OpenVLC board, the low-power LED and study low-power LED-to-LED communication, where a single LED is used to both transmit and receive along with a few basic electronic components. This design has been proved to be resilient to ambient light interference without additional electronic processing [3], and could be well suited for a communication network of consumer devices with LED front-end. We adopt off-the-shelf electronic components to implement a basic physical layer. The block diagram of transceiver is shown in Fig. 7(left). It includes a TransImpedance Amplifier (TIA) and an Analog-to-Digital Converter (ADC) for reception, a tri-state-output buffer and ancillary circuitry for switching between transmission and reception.

A prerequisite to enable the intra-frame bidirectional transmission is that the nodes can swiftly switch between TX mode and RX mode on a symbol basis. In our implementation, a software-defined TX/RX switch is used to switch the LED between TX and RX through the GPIO pins:

- in **TX mode**, encoded signals are amplified by the tri-state buffer and then fed to the forward-biased LED for light emission;
- in **RX mode**, light signal is received by the LED and then the received small photocurrent is amplified by the TIA.

Finally, an ADC converts the output analog signals to digital signals, which are then sent to the decoder through the Serial Peripheral Interface (SPI).

Through the TX/RX switch and the tri-state buffer, the LED can switch between being TX and RX modes with low latency.

[3]http://beagleboard.org/Products/BeagleBone+Black

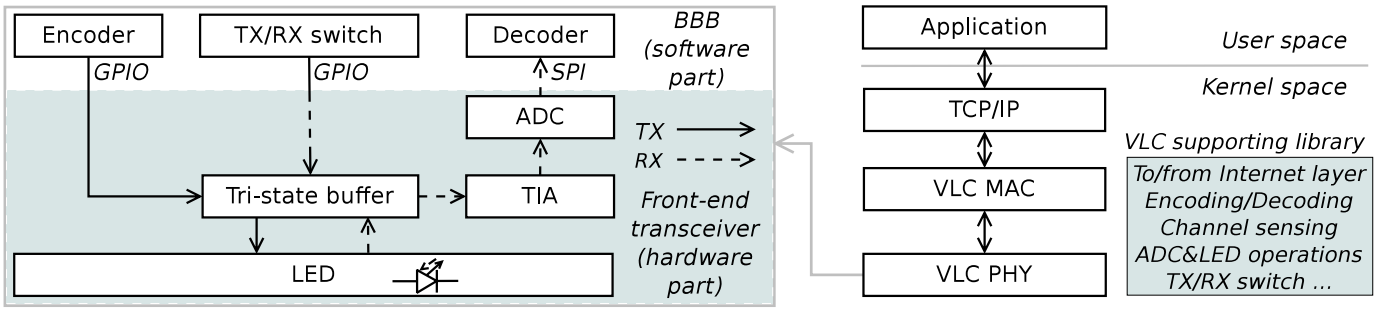

Fig. 7. The diagram of our implementation: left) the front-end transceiver; right) the communication stack.

Preamble	SFD	Length	Dst	Src	Protocol	Payload	CRC
3 Bytes	1 B	2 B	2 B	2 B	2 B	0-MAX B	2 B

Fig. 8. Frame format of DATA and ACK: Length $> 0 \iff$ DATA; Length $= 0 \iff$ ACK.

This makes it possible to enable the intra-frame bidirectional transmission presented in Sec. III-B.

B. Software

The operating system running within the BBB board is the Debian Linux Distribution. Fig. 7(right) illustrates the software stack of the implementation, where the VLC MAC and VLC PHY are built based on the primitive functions we implement. These functions include writing a symbol to the LED, reading a symbol from the ADC, coding/decoding, preamble detection, TX/RX switching, and so on.

In our implementation, there are two types of frames in the MAC layer, DATA and Acknowledgement (ACK). The DATA frame structure and octets each field occupies are shown in Fig. 8. Distinguishing DATA and ACK frames is through the length of frame body (payload): if the frame has no payload (i.e., "Length" $= 0$), it is an ACK frame. Otherwise, it is a DATA frame. Each DATA frame can carry a payload from 0 to MAX (a predefined value) bytes. The MAC destination and source addresses that follow the "Length" field each occupies 2 bytes. The 2-byte filed "Protocol" identifies the upper layer protocol encapsulated in the payload. The fields from "Length" to "Protocol" form the MAC frame header. A two-octet Cyclic Redundancy Check (CRC) over the frame header and payload is appended to the end of payload. The Reed-Solomon correcting code over the MAC header, payload and CRC is added to the end of each DATA frame. A three-octet preamble is appended to the beginning of each frame for synchronization.

VI. Experimental Evaluation

In this section, we evaluate the proposed protocols through experiments. We run Debian Linux System with kernel version 3.8.13 and the Xenomai patch within the BBB board. The electronic devices used in our implementation are summarized in Table III. We use a symbol period of 20 μs for both LOW and HIGH symbols and the (232,200) Reed-Solomon code at each node. Different to a primary frame, an embedded frame is coded with OOK modulation without the Manchester code (bit "0" is mapped to symbol LOW and bit "1" to symbol HIGH). Note that in the experiments we use multiple narrow-FOV LEDs to emulate a wider-FOV LED when necessary. All the experiments are carried out in an indoor environment with normal office lights on where the noise level is around 90 lux.[4] The value of `maxNumLOW` introduced in Algorithm 2 is initiated to 20. Besides, for simplicity and unless otherwise specified, the bits "0" and "1" in the experiments are set to be evenly distributed within the payload of frames (i.e., the percentage of bit "1" in the payload is 50%).

TABLE III
Electronic Devices Used in the Implementation

Model	Description
HLMP-EG08-YZ000	Low-power 5 mm red LED with a Field-Of-View (FOV) of 8°
SN74HCT125N	8-bit buffer with tri-state outputs
TLC272CP	Transimpedance operational amplifier
MCP3008	10-bit analog-to-digital converter

A. Performance With Embedded Channels

Point-to-Point Link: We evaluate the MAC layer saturation throughput of a point-to-point link without and with the intra-frame bidirectional transmissions, where the nodes are within the FOV of each other. The saturation throughput is achieved under the setting that nodes always have data to transmit. Throughput versus the per-primary-frame payload is shown in Fig. 9(a), where the payload varies from 50 to 1000 bytes. First we can observe that the results from the experiments and the analysis match with each other very well. As expected, the throughputs under both protocols in consistent with the payload, *e.g.*, with the intra-frame bidirectional transmission, the saturation throughput is around 11 kb/s when the payload is 50 bytes, while the throughput achieves a value of 30 kb/s when the payload increases to 1000 bytes. Another observation from Fig. 9(a) is that the performance with embedded channel outperforms greatly the performance without embedded channel when the payload is long, *e.g.*, when the payload is 1000 bytes, the throughput of the former is about 150% of that of the latter. This achievement comes from the intra-frame bidirectional transmission. The throughputs of

[4]The noise floor is measured by an Android phone (Huawei MATE1).

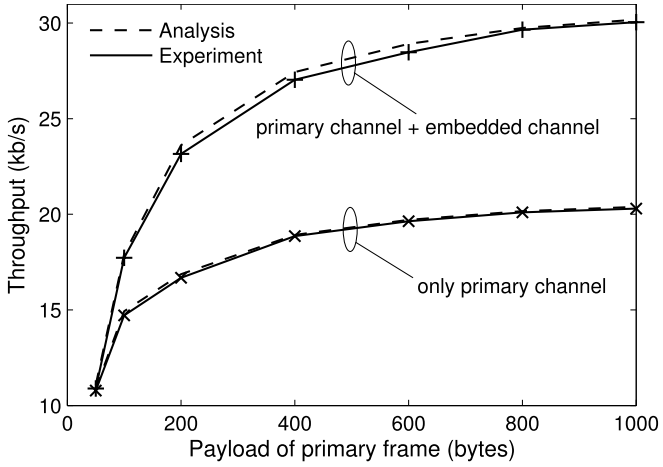

(a)

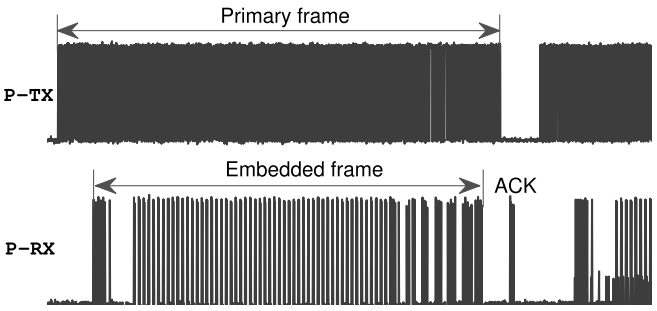

(b)

Fig. 9. Evaluation results of a point-to-point link. (a) Saturation throughput. *The primary channel is P-TX→P-RX; the embedded channel is P-RX→P-TX.* (b) Oscilloscope snapshot *(the primary/embedded/ACK frames shown here are transmitted by their corresponding nodes, not received).*

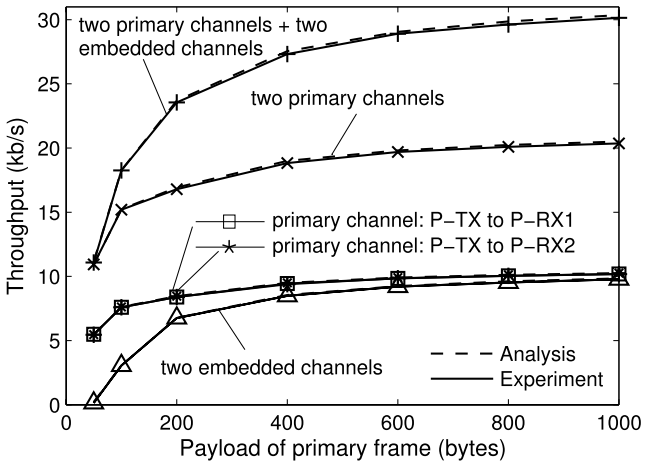

(a)

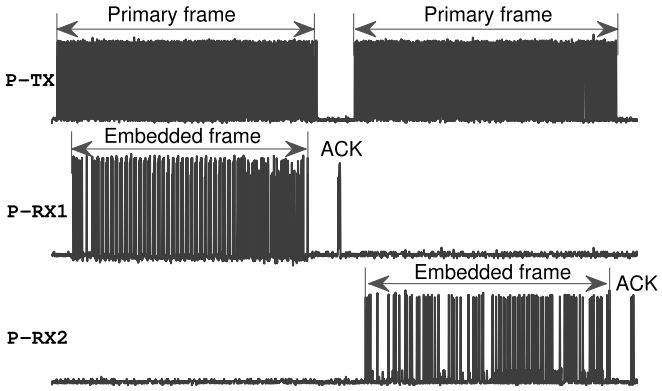

(b)

Fig. 10. Evaluation results of a three-node network. (a) Saturation throughput. *The two primary channels are P-TX→P-RX1 and P-TX→P-RX2; the two embedded channels are P-RX1→P-TX and P-RX2→P-TX.* (b) Oscilloscope snapshot *(primary/embedded/ACK frames shown here are transmitted by their corresponding nodes, not received).*

the two protocols are almost the same when the payload is 50 bytes. This is because the transmission of an effective embedded frame is nearly impossible when the payload of a primary frame is too short. An oscilloscope snapshot of the protocol with embedded channel is shown in Fig. 9(b), where we can see clearly the interaction of nodes as well as the transmission of embedded frames.

Three-Node Network: In this scenario, one node acts a base station and keeps sending data alternately to the other two nodes (*i.e.*, the base station uses the round-robin scheduling algorithm). Again, we can observe from Fig. 10(a) that the result from experiments matches well with that from analysis. As expected, we can see from the figure that the throughputs at the two receivers are similar under various frame payloads. Also, the throughput gain of the protocol with the embedded channel over the protocol without it increases with the frame payload. This gain achieves a value of 50% when the payload is 1000 bytes. The interactions between these nodes are illustrated by the oscilloscope snapshot in Fig. 10(b).

Four-Node Network: The performance of a four-node network is also evaluated. The settings can be referred to the left subfigure of Fig. 1, where the four nodes A, B, C, and D act as P-TX, P-RX, S-TX, and S-RX, respectively. The oscilloscope snapshot of the interactions between these nodes is presented in Fig. 11(b). We can see clearly that three intra-frame concurrent transmissions are obtained. The corresponding saturation throughputs of this network are presented in Fig. 11(a). We observe that, for both protocols, the throughput increases with the payload size. The protocol with embedded channels starts to outperform greatly the protocol without embedded channels after the payload is larger than 50 bytes. The maximal throughput gain is around 100% after the payload reaches 1000 bytes, twice as large as the gains of the point-to-point link and three-node network. The reason for this is that, in the four-node network, an additional intra-frame transmission is enabled between the S-TX and S-RX.

B. Ad-Hoc Scenario

In this part we evaluate the proposed CSMA/CD-HA protocol through experiments. As in the numerical results presented in Sec.IV-C, we compare the performance of CSMA/CD-HA with those of CSMA/CA and CSMA/CD. In all the protocol, an 8-symbol period is used for channel sensing,

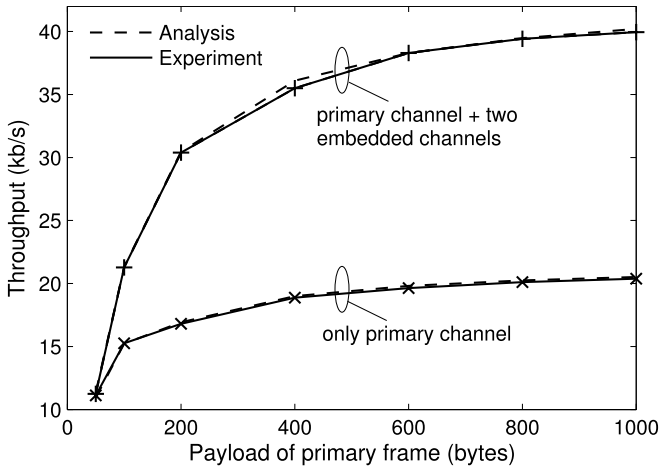

(a)

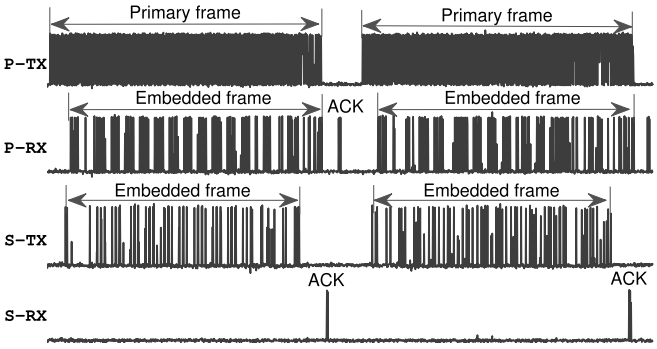

(b)

Fig. 11. Evaluation results of a four-node network. (a) Saturation throughput. *The primary channel is P-TX→P-RX; the two embedded channels are P-RX→P-TX and S-TX→S-RX*. (b) Oscilloscope snapshot *(primary/embedded/ACK frames shown here are transmitted by their corresponding nodes, not received).*

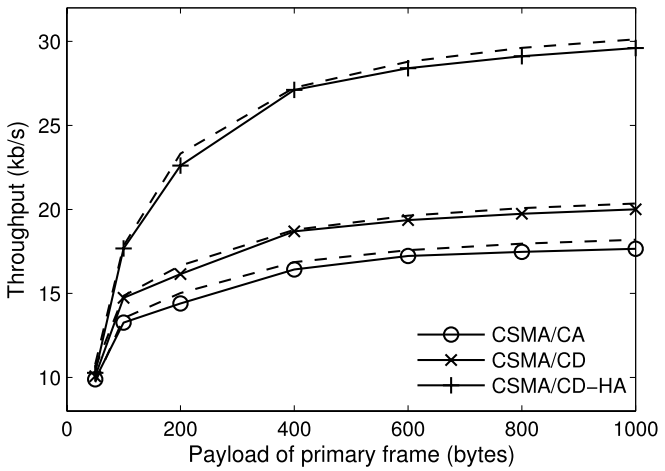

Fig. 12. Evaluation results of a three-node network (*corresponding analytical results are represented by the dash lines*).

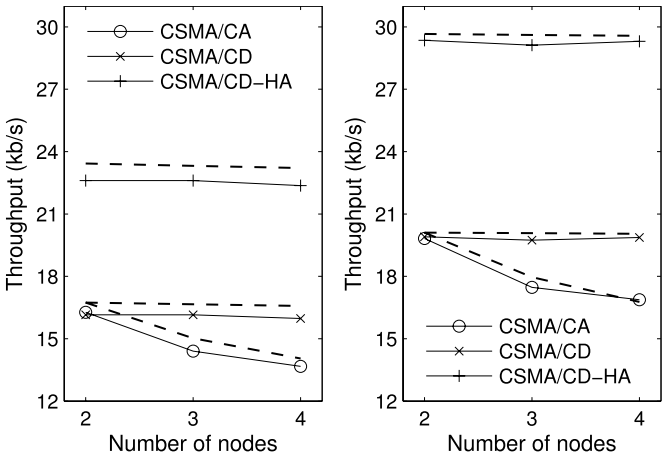

(a) (b)

Fig. 13. Evaluation results of an ad-hoc network with different payloads of primary frames and different number of nodes (*corresponding analytical results are represented by the dash lines*). (a) Payload = 200 bytes. (b) Payload = 800 bytes.

i.e., to determine whether the channel is clear or not. The minimum and maximum value of the contention window are set to 4 and 32, respectively. The maximum frame retransmission times is set to 4. Both CSMA/CD and CSMA/CD-HA uses the same backoff mechanism as in the traditional CSMA/CA protocol. While transmitting, a node adopting CSMA/CD or CSMA/CD-HA stops the ongoing transmission if a collision is detected.

Three-Node Network Without Hidden Nodes: The saturation throughput in a three-node network without hidden nodes is shown in Fig. 12. The payload is set to vary from 50 to 1000 bytes. As in Section VI-A, we can observe that the throughputs with different protocols increase consistently with the payload, and the experimental results match well with the analytical results. The CSMA/CD is observed to outperform CSMA/CA, as shown in [3]. The throughput with CSMA/CD-HA outperforms that with CSMA/CD, due to the enabled embedded channel. Both of them can achieve higher throughputs than CSMA/CA, because they can detect collisions during the frame transmission.

Networks With Different Number of Nodes: The saturation throughput under different number of nodes is shown in Fig. 13, where nodes varies from 2 to 4, and payload changes between 200 and 800 bytes. First we can observe that results from experiments and analysis match well with each other. We also notice that the throughput with CSMA/CA decreases as the number of nodes increases, while the throughputs with the CSMA/CD and CSMA/CD-HA are almost not affected. Besides, we can see clearly from the results that CSMA/CD-HA can achieve much higher throughput than CSMA/CA and CSMA/CD, independent of the number of nodes and payload length. For example, in Fig. 13(b) and when there are 4 nodes, the throughput gains of CSMA/CD-HA over CSMA/CA and CSMA/CD are around 70% and 50%, respectively.

Three-Node Network With Hidden Nodes: We also evaluate a three-node network with hidden nodes, similar to the illustration shown in the right sub-figure of Fig. 1. The experiments are carried out in non-saturation scenarios. Under a scenario with specific-length frames, the inter-frame interval (interval between a node finishes transmitting a frame and that node

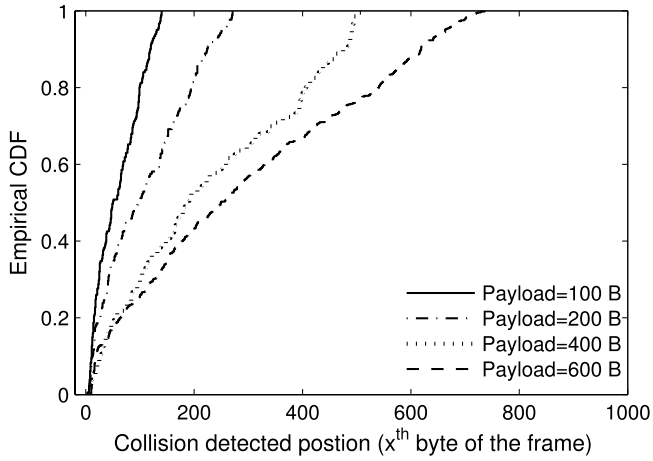

(a)

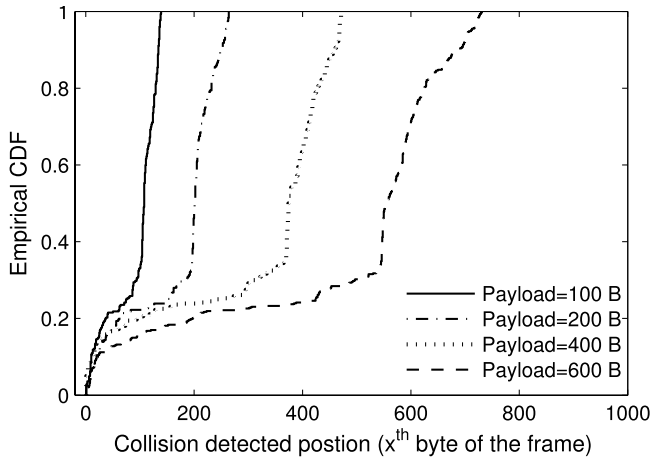

(b)

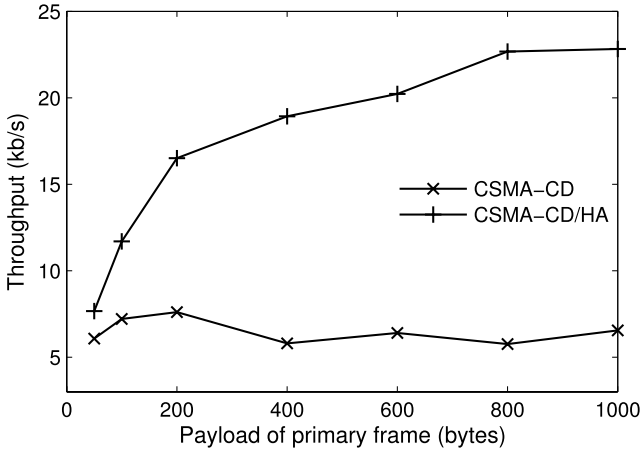

(c)

Fig. 14. Evaluation results of the three-node network with hidden nodes. (a) Collision position of CSMA/CD. (b) Collision position of CSMA/CD-HA. (c) Non-saturation throughput.

has a new frame for transmission) is set to a value doubles the time taken to transit one of that specific-length frames at the PHY layer. We compare the CSMA/CD-HA with the CSMA/CD protocol. The position where a collision is detected within each collided frame is presented in Fig. 14. We can observe from Fig. 14(a) that under CSMA/CD, the collisions occurs at positions that are almost evenly distributed within the frame. This is because the two TXs can not hear each other's transmission. In turn, this can cause a collision at any part of the ongoing transmitting frames. However, the collisions under CSMA/CD-HA occur either at the beginning or at the end of collided frames, as shown in Fig. 14(b). This is due to the fact that a RX starts sending an embedded frame after it receives the source address of the corresponding primary frame, and finishes sending the embedded frame before the whole primary frame is fully transmitted (as illustrated in Fig. 4). Although there are still collisions caused by the hidden node under CSMA/CD-HA, the number of collisions is actually reduced greatly. This is shown in Fig. 14(c), where the saturation throughput versus frame payload is presented. We can observe that CSMA/CD-HA always outperforms CSMA/CD greatly independent of the frame payloads, and the throughput gain can be up to three times higher when the frame payload is set to 1000 bytes.

C. Bit Scrambling

The performance of the intra-frame bidirectional transmission can be weakened if:

- the payload of a primary frame has two many "1", or
- the embedded frame payload has long sequences of bit "0."

In the first case, the payload of an embedded frame would be shorten significantly. In the second case, the system would be less resilient to collisions and hidden nodes. Therefore the P-TX may stop transmitting the ongoing primary frame. To solve these problems, we adopt the *bit scrambling* technique over the payloads of both primary and embedded frames. We choose bit scrambling because it has the ability to convert any sequences into seemingly random sequences, thus avoiding long sequences of bits of the same value [29].

We use a 16-bit Fibonacci Linear-Feedback Shift Register (LFSR) to implement the bit scrambling. The feedback taps are at the 16th, 14th, 13th, and 11th bits, *i.e.*, the feedback polynomial is $x^{16} + x^{14} + x^{13} + x^{11} + 1$. The nonzero state `0xACD1U` is chosen as a start state of the 16-bit Fibonacci LFSR. The experiments are carried out on a point-to-point link. The payload of primary frames is fixed to 800 bytes, while the percentage of bit "1" within payload varies within the range $[1/8, 1/4, ..., 3/4, 7/8]$. We compare the performance under three different cases: i) no embedded channel; ii) one embedded channel; iii) bit scrambling. In the last case, we use a dynamic scrambling approach. The scrambler in the primary frame is enabled only if the percentage of bit "1" within the payload is above 50%. The idea of this approach is to dynamically take advantage of longer set of bit "1"s to increase the system throughput. To implement this, we use a bit of the SFD to inform the receiver whether the scrambler is enabled or not in the current frame.

The evaluation results are shown in Fig. 15. As previously, we can notice that the experimental results match well with the analytical results. As expected, the throughput with no embedded channel is not sensitive to the percentage of bit "1" at all. However, the throughput with one embedded channel

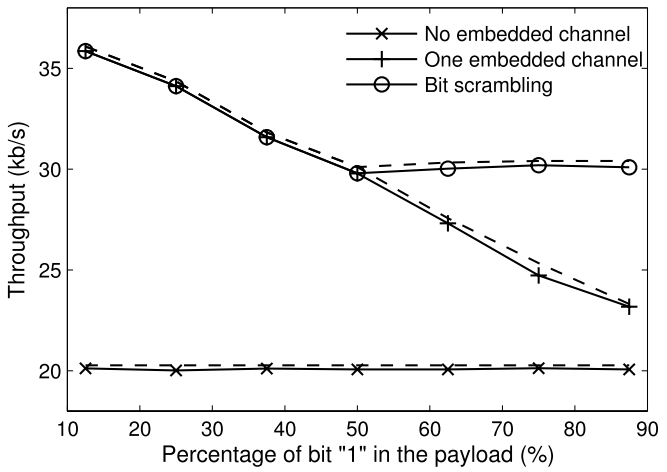

Fig. 15. Evaluation results of a point-to-point link with bit scrambling (*corresponding analytical results are represented by the dash lines*).

depends heavily on the percentage of bit "1", *e.g.,* when $1/8$ of the bits within the payload are "1", the throughput can reach up to 36 kb/s; while it drops to 23 kb/s when the percentage of bit "1" becomes $7/8$. Due to the bit scrambling's ability of converting any sequences to seemingly random sequences, the throughput with bit scrambling can keep stable around 30 kb/s after the percentage of bit "1" in the payload exceeds 50%.

VII. Conclusion

In this paper, we introduced the intra-frame bidirectional transmission approach for visible light communication networks using one optical antenna for transmission and reception. Based on it, we presented the design, analysis, implementation, and performance evaluation of the CSMA/CD-HA MAC protocol. We implemented the protocol in a software-defined embedded platform, solved practical challenges, and showed its superior ability to detect collisions and alleviate hidden nodes, thus boosting the system throughput.

Appendix

Let $b(t)$ and $s(t)$ be the stochastic process representing the backoff window size and backoff state for a given node at slot time t, respectively. Let $b_{i,k} = \lim_{t\to\infty}\{s(t) = i, b(t) = k\}, 0 \le i \le m, 0 \le k \le W_i - 1$ be the stationary distribution of the Markov chain, where m is the maximal backoff stage and W_i is the maximal backoff window size of the ith backoff stage. Besides, let p denote the collision probability during a frame's transmission, and τ be the probability a node transmits in an arbitrary time slot. Following the analysis in [26], we can get

$$\begin{cases} p = 1-(1-\tau)^{n-1} \\ \tau = \dfrac{1-p^{m+1}}{1-p}\cdot b_{0,0} \\ b_{0,0} = \dfrac{2(1-2p)(1-p)}{W_0(1-p)[1-(2p)^{m+1}]+(1-2p)(1-p^{m+1})} \end{cases} \tag{7}$$

Based on Eqs. (7), variables τ and p can be solved numerically. Note that τ and p satisfy $0 < \tau < 1$ and $0 < p < 1$.

Saturation Throughput: Let P_{tr} be the probability that the channel is busy (at least one node is transmitting) in the considered slot time, then we have

$$P_{tr} = 1-(1-\tau)^n \tag{8}$$

The probability P_f that a frame transmission is successful is given by

$$P_f = n\tau(1-\tau)^{n-1} \tag{9}$$

Moreover, the probability P_c that a collision occurs during a frame's transmission is expressed as

$$P_c = P_{tr} - P_f = 1-(1-\tau)^n - n\tau(1-\tau)^{n-1} \tag{10}$$

The time for a successful transmission T_f is given by

$$T_f = T_h + E[T_p] + \delta + T_s + T_a + \delta + T_l \tag{11}$$

Let T_c^{ca} and T_c^{cd} be the collision time under the CSMA/CA and CSMA/CD-HA, respectively. We have

$$T_c^{ca} = T_h + E[T_p] + \delta + T_l \tag{12}$$

and

$$T_c^{cd} = T_h + E[T_p'] + \delta + T_l \tag{13}$$

Note that $E[T_p'] \ll E[T_p]$.

Let S_{ca} denote the saturation throughput under CSMA/CA. Then S_{ca} can be written as

$$S_{ca} = \frac{P_f E[L_p]}{(1-P_{tr})\sigma + P_f T_f + P_c T_c^{ca}} \tag{14}$$

where σ is the duration of an empty time slot.

Similarly, let S_{cd} and S_{cd_ha} be the saturation throughputs under CSMA/CD and under CSMD/CD-HA (with embedded transmission), respectively. We have

$$S_{cd} = \frac{P_f E[L_p]}{(1-P_{tr})\sigma + P_f T_f + P_c T_c^{cd}} \tag{15}$$

$$S_{cd\_ha} = \frac{P_f (E[L_p] + E[L_{em}])}{(1-P_{tr})\sigma + P_f T_f + P_c T_c^{cd}}. \tag{16}$$

References

[1] Q. Wang and D. Giustiniano, "Communication networks of visible light emitting diodes with intra-frame bidirectional transmission," in *Proc. ACM CoNEXT*, 2014, pp. 21–28.

[2] P. Dietz, W. Yerazunis, and D. Leigh, "Very low-cost sensing and 843 communication using bidirectional LEDs," in *Proc. ACM UbiComp*, 2003, pp. 175–191.

[3] D. Giustiniano, N. O. Tippenhauer, and S. Mangold, "Low-complexity visible light networking with LED-to-LED communication," in *Proc. IFIP Wireless Days (WD)*, Nov. 2012, pp. 1–8.

[4] D. Bharadia, E. McMilin, and S. Katti, "Full duplex radios," in *Proc. ACM SIGCOMM*, 2013, pp. 375–386.

[5] D. Tsonev, S. Videv, and H. Haas, "Light fidelity (Li-Fi): Towards all-optical networking," in *Proc. SPIE 9007*, 2013, pp. 900702-1–900702-10.

[6] S. Wu, H. Wang, and C.-H. Youn, "Visible light communications for 5G wireless networking systems: From fixed to mobile communications," *IEEE Netw.*, vol. 28, no. 6, pp. 41–45, Nov./Dec. 2014.

[7] T. Hao, R. Zhou, and G. Xing, "COBRA: Color barcode streaming for smartphone systems," in *Proc. ACM MobiSys*, 2012, pp. 85–98.

[8] W. Hu, H. Gu, and Q. Pu, "LightSync: Unsynchronized visual communication over screen-camera links," in *Proc. ACM MobiCom*, 2013, pp. 15–26.

[9] C. B. Liu, B. Sadeghi, and E. W. Knightly, "Enabling vehicular visible light communication (V^2LC) networks," in *Proc. ACM VANET*, 2011, pp. 41–50.
[10] S.-H. Yu, O. Shih, H.-M. Tsai, N. Wisitpongphan, and R. Roberts, "Smart automotive lighting for vehicle safety," *IEEE Commun. Mag.*, vol. 51, no. 12, pp. 50–59, Dec. 2013.
[11] L. Li, P. Hu, C. Peng, G. Shen, and F. Zhao, "Epsilon: A visible light based positioning system," in *Proc. NSDI*, 2014, pp. 331–343.
[12] Y.-S. Kuo, P. Pannuto, K.-J. Hsiao, and P. Dutta, "Luxapose: Indoor positioning with mobile phones and visible light," in *Proc. ACM MobiCom*, 2014, pp. 447–458.
[13] Z. Yang, Z. Wang, J. Zhang, C. Huang, and Q. Zhang, "Wearables can afford: Light-weight indoor positioning with visible light," in *Proc. ACM MobiSys*, 2015, pp. 317–330.
[14] H.-Y. Lee *et al.*, "RollingLight: Enabling line-of-sight light-to-camera communications," in *Proc. ACM MobiSys*, 2015, pp. 167–180.
[15] A. Wang *et al.*, "InFrame++: Achieve simultaneous screen-human viewing and hidden screen-camera communication," in *Proc. ACM MobiSys*, 2015, pp. 181–195.
[16] T. Li, C. An, X. Xiao, A. T. Campbell, and X. Zhou, "Real-time screen-camera communication behind any scene," in *Proc. ACM MobiSys*, 2015, pp. 197–211.
[17] *IEEE Standard for Local and Metropolitan Area Networks—Part 15.7: Short-Range Wireless Optical Communication Using Visible Light*, IEEE Standard 802.15.7-2011, Sep. 2011, pp. 1–309.
[18] Q. Wang, D. Giustiniano, and D. Puccinelli, "OpenVLC: Software-defined visible light embedded networks," in *Proc. 1st ACM Workshop VLCS*, Sep. 2014, pp. 15–20.
[19] Q. Wang, D. Giustiniano, and D. Puccinelli, "An open source research platform for embedded visible light networking," *IEEE Wireless Commun.*, vol. 22, no. 2, pp. 94–100, Apr. 2015.
[20] Q. Wang, D. Giustiniano, and O. Gnawali, "Low-cost, flexible and open platform for visible light communication networks," in *Proc. 2nd ACM Workshop HotWireless*, 2015, pp. 31–35.
[21] H. Chun *et al.*, "Demonstration of a bi-directional visible light communication with an overall sum-rate of 110 Mb/s using LEDs as emitter and detector," in *Proc. IEEE Photon. Conf. (IPC)*, Oct. 2014, pp. 132–133.
[22] J. I. Choi, M. Jain, K. Srinivasan, P. Levis, and S. Katti, "Achieving single channel, full duplex wireless communication," in *Proc. 16th ACM MobiCom*, 2010, pp. 1–12.
[23] M. Jain *et al.*, "Practical, real-time, full duplex wireless," in *Proc. ACM MobiCom*, 2011, pp. 301–312.
[24] K. I. X. Lin and K. Hirohashi, "High-speed full-duplex multiaccess system for LED-based wireless communications using visible light," in *Proc. Int. Symp. Opt. Eng. Photon. Technol. (OEPT)*, 2009, pp. 1–5.
[25] J. Zhang, X. Zhang, and G. Wu, "Dancing with light: Predictive in-frame rate selection for visible light networks," in *Proc. IEEE INFOCOM*, Apr./May 2015, pp. 2434–2442.
[26] G. Bianchi, "Performance analysis of the IEEE 802.11 distributed coordination function," *IEEE J. Sel. Areas Commun.*, vol. 18, no. 3, pp. 535–547, Mar. 2000.
[27] D. Malone, K. Duffy, and D. Leith, "Modeling the 802.11 distributed coordination function in nonsaturated heterogeneous conditions," *IEEE/ACM Trans. Netw.*, vol. 15, no. 1, pp. 159–172, Feb. 2007.
[28] O. Ekici and A. Yongacoglu, "IEEE 802.11a throughput performance with hidden nodes," *IEEE Commun. Lett.*, vol. 12, no. 6, pp. 465–467, Jun. 2008.
[29] R. D. Gitlin, J. F. Hayes, and S. B. Weinstein, *Data Communications Principles*. New York, NY, USA: Springer, 1992.

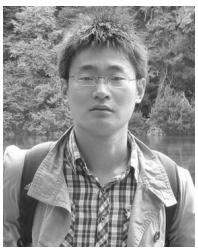

Qing Wang (S'13) received the bachelor's and master's degrees from the University of Electronic Science and Technology of China, Chengdu, China, in 2008 and 2011, respectively, and the master's degree from the University Carlos III of Madrid, Spain, in 2012. He is currently pursuing the Ph.D. degree with the IMDEA Networks Institute and the University Carlos III of Madrid. His interests include visible light communication, device-to-device communication, stochastic optimization, and performance evaluation.

Domenico Giustiniano (S'06–M'13) received the Ph.D. degree in telecommunication engineering from the University of Rome Tor Vergata, Italy, in 2008. He was a Senior Researcher and Lecturer with ETH Zurich and a Post-Doctoral Researcher with Disney Research Zurich and Telefonica Research Barcelona. He is currently a Research Associate Professor with the IMDEA Networks Institute and a Leader of the Pervasive Wireless Systems Group. He has authored over 60 international papers and holds five patents. He devotes most of his current research to emerging areas, including visible light communication networks, mobile indoor localization, and collaborative spectrum sensing.